

# Interplay of Structure and Dynamics in Macromolecular and Supramolecular Systems

Hans Wolfgang Spiess\*

Max Planck Institute for Polymer Research, 55128 Mainz, Germany

Received March 17, 2010; Revised Manuscript Received May 14, 2010

**ABSTRACT:** In recent years major advances in generating, characterizing, and understanding macromolecular and supramolecular systems have been achieved. This has led to an enormous variety and complexity in polymer science. The traditional separation in terms of structure vs dynamics, crystalline vs amorphous, or experiment vs theory is increasingly overcome. As far as characterization of such materials is concerned, no experimental or theoretical/simulation approach alone can provide complete information. Instead, a combination of techniques is called for, and conclusions should be supported by results provided by complementary techniques. This Perspective discusses the kind of information that can be obtained by advanced solid state NMR and EPR spectroscopy, combined and/or compared with X-ray and neutron scattering as well as dielectric spectroscopy and computer simulation. The multi-technique approach is demonstrated by a number of examples including morphology, defects, heterogeneities in time scale and amplitude of motion, and local and collective dynamics in polymers of different architectures, biomacromolecules, and hybrid systems.

## Introduction

In soft matter, function of complex synthetic as well as natural systems is often achieved by separating regions of order and disorder. For entropic reasons such phase separation happens spontaneously even in macromolecules with chemically identical repeat units, leading to semicrystalline polymers and even more so in polymer systems composed of different repeat units, i.e., polymer blends or copolymers.<sup>1,2</sup> Incompatibility of building blocks, e.g., backbone and side groups in macromolecules, or noncovalent interactions, such as hydrogen bonds, ionic forces, or  $\pi$ – $\pi$  interactions, lead to self-organization.<sup>3</sup> In the resulting structures the different units are spatially separated and may display vastly different dynamics. This is even more pronounced if organic and inorganic residues are combined. Even if highly ordered on a local scale, such systems often do not crystallize. Therefore, their atomic resolution structures cannot be determined by conventional X-ray or neutron scattering techniques. In order to provide insight into the organization of such materials, advanced methods of characterization should be able to probe both structure and dynamics simultaneously. Traditionally, however, the determination of structure and the elucidation of dynamics of matter are considered separately. With the advancement of characterization techniques, however, this separation becomes more and more artificial. Instead, elucidation of the structure can facilitate the understanding of dynamic properties and *vice versa*. In fact, determination of the molar mass by dynamic light scattering,<sup>4</sup> well-established in the polymer field, provides an instructive example as there the size of the macromolecule (structure) is determined from measuring their translational diffusion, i.e., a dynamic phenomenon. In liquid crystals,<sup>5</sup> the degree of alignment of the residues (structure) is conveniently determined from the reduction of an anisotropic interaction, e.g., dipole–dipole coupling in NMR by restricted molecular dynamics. As functional supramolecular materials often display liquid crystalline phases, this provides a convenient way of at least partially determining their structure.

\*E-mail: spiess@mpip-mainz.mpg.de.

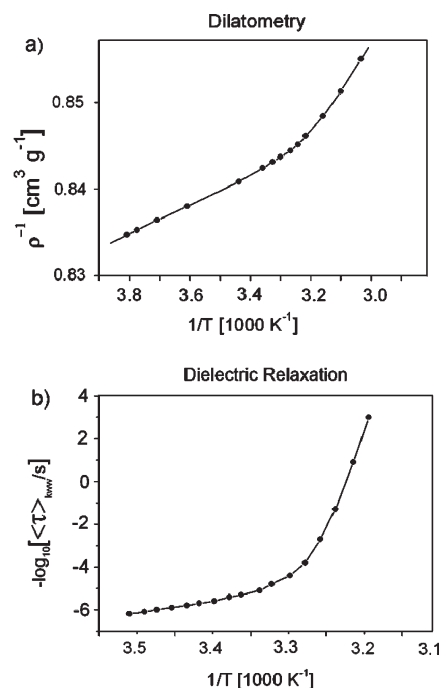


**Figure 1.** Glass transition of poly(vinyl acetate). Comparison of (a) density change measured by dilatometry<sup>6</sup> and (b) changes in molecular dynamics detected by dielectric spectroscopy.<sup>7</sup>

In fact, slow molecular dynamics are extremely sensitive to even the slightest differences in structure. Polymer behavior at the glass transition is a well-known example. In Figure 1 the density change of poly(vinyl acetate) during the glass transition<sup>6</sup> is compared with the change in molecular dynamics as revealed by broad-band dielectric spectroscopy.<sup>7</sup> Within a temperature range of 30 K, the density changes by 2.1%, whereas the dynamics spans a range of 8 orders of magnitude! Thus, slow dynamics monitors the slightest structural changes and can be used to detect such changes,



Hans Wolfgang Spiess, born in 1942, received his doctoral degree in physical chemistry in 1968 from the University of Frankfurt with H. Hartmann. After a postdoctoral stay at Florida State University (with R. K. Sheline), he returned to Germany in 1970 and joined the Max Planck Institute for Medical Research (with K. H. Hausser), taking part in the rapid development of novel NMR techniques for studying molecular motion in liquids and solids. In 1978, he finished his habilitation in physical chemistry at the University of Mainz in the group of H. Sillescu. Subsequently, he held professorships of physical chemistry at the University of Münster (1981–1982) and macromolecular chemistry at the University of Bayreuth (1983–1984). In 1984, he was appointed a director of the newly founded Max Planck Institute for Polymer Research in Mainz. His research interests include the development of magnetic resonance techniques for elucidating the structure, dynamics, phase behavior, and order of synthetic macromolecules and supramolecular systems. He applies these methods to the study of new polymer materials to relate their microscopic and macroscopic behavior. Spiess has served as chairman of the European Polymer Federation (1991–1992) and as chairman of the Capital Investment Committee of the German Science Foundation (1994–1996). From 1999 until 2005 he has been a member of the Scientific Council of the Federal Republic of Germany. His achievements have been honored by several distinctions, including the Leibniz Prize of the German Research Foundation in 1987, the European Ampere Prize, the Liebig Medal of the German Chemical Society, the Award of the Society of Polymer Science (Japan) in 2002, the Walther Nernst Medal of the German Bunsen Society for Physical Chemistry in 2007, and the Paul J. Flory Research Prize in 2010. He is doctor honoris causa of the Technical University of Cluj-Napoca, Romania (1997), and of Adam Mickiewicz University, Poznan, Poland (1998).

even when conventional tools of structural characterization reach their limits.

If structural information on a molecular level is sought, *site selectivity* is required. Moreover, for macroscopic organization, mechanical properties, and transport of ions or charges in highly viscous materials or even solids “slow” dynamics on time scales longer than microseconds are particularly relevant. While several techniques meet one or the other requirement for elucidating structure and/or dynamics, *NMR spectroscopy* stands out as it meets all of them,<sup>8</sup> and rapid development of the NMR methods is still ongoing. It should be acknowledged, however, that no single technique can provide the required information. Instead, a combination of complementary methods is required. This also includes combination of experimental techniques and computer simulation in its remarkable development.<sup>9</sup> Therefore, this Perspective describes new developments in NMR spectroscopy as applied to macromolecular and supramolecular systems, relates this information to that obtained by other techniques, in particular scattering, and describes specific examples of combined studies in areas recently identified as challenges and opportunities in macromolecular science.<sup>10</sup>

### Experimental Methods for Elucidating the Interplay between Structure and Dynamics

**NMR Spectroscopy.** NMR spectroscopy is remarkably versatile and, therefore, is widely applied in many fields of science, in particular physics, chemistry, biology, materials

science, and last but not least medicine.<sup>11</sup> NMR is nondestructive, sample preparation is easy, and the possibility to observe different nuclei and isotopes provides extreme structural and site selectivity.<sup>12</sup> Moreover, dynamic features can be studied over many decades of characteristic times, from picoseconds to minutes,<sup>8</sup> and length scales from interatomic distances in the 100 pm range up to a meter or so in NMR imaging.<sup>13</sup> The wealth of information accessible by NMR spectroscopy results from the fact that a variety of interactions of the nuclear spins with their surroundings can be exploited. The unique information about relationships of distinguishable units can be established in space and time by multidimensional and multiple quantum NMR spectroscopy.<sup>8,12,14</sup>

In particular, the structure of polymers and other supramolecular systems can be elucidated along several routes. The chemical shift provides the basis of site selectivity and geometric parameters such as internuclear distances as well as dihedral angles are encoded in the dipole–dipole and the *J*-coupling. Of the great variety of molecular motions possible in polymers, rotations have the most pronounced effects on NMR spectra and relaxation parameters, because the spin interactions have a well-defined angular dependence. But conformational dynamics and translational motions can be tackled as well. The anisotropic nuclear spin interactions also offer a means to probe the alignment of residues in partially ordered systems such as drawn fibers<sup>15</sup> or oriented liquid crystals (see above).<sup>5</sup>

Traditionally NMR spectroscopy is divided in high resolution liquid state and low resolution solid state NMR.<sup>8,12</sup> Nowadays, however, this division is no longer appropriate, as anisotropic spin interactions are also exploited in liquid state NMR, e.g., in structure determination of proteins in solution.<sup>16</sup> Moreover, in polymers and supramolecular systems, liquid and solid states are not clearly separated, e.g., in the amorphous state in the vicinity of the glass transition. Thus, the methodologies converge, albeit the technical differences should not be ignored. Indeed, application of NMR spectroscopic methods from protein NMR to study synthetic polymers in solution provides unambiguous atomic connectivity information in the polymer backbone which facilitates analysis of comonomer composition, stereosequence distribution, and branching structures.<sup>17</sup> As several reviews on new developments of NMR on bulk polymers and supramolecular systems are available,<sup>18–20</sup> we refrain from describing the techniques in detail again. Instead, we have collated the information accessible through the anisotropic spin interactions in Table 1.

**X-ray and Neutron Scattering.** Scattering is a particularly powerful tool in polymer science. While X-ray scattering<sup>21</sup> is most valuable for elucidation of the structure, neutron scattering in addition provides information on the geometry and time scale of molecular motions.<sup>22</sup> Remarkable similarities exist between quasielastic neutron scattering and multidimensional exchange NMR,<sup>23,8</sup> as both methods provide information about the geometry (amplitude) and the time scale of molecular motion independently, albeit on different time scales. In the case of *translational* motion incoherent neutron scattering and pulsed field gradient NMR even probe the same dynamic structure function.<sup>24,25</sup> Moreover, combination of pulsed field gradient NMR and electrophoresis NMR permits the direct observation of counterion condensation in polyelectrolytes.<sup>26</sup> With the availability of advanced neutron sources, the time scale accessible to neutron scattering has recently been extended to longer times,<sup>27</sup> which offers new possibilities in studies of polymer physics.<sup>28</sup> Remarkably a similar analogy exists between the so-called two-dimensional DECODER NMR<sup>29</sup> and pole figure analysis in X-ray scattering on partially

**Table 1. Interactions of Nuclei among Themselves and with Their Surroundings, Which Provide the Basis for Elucidating Structure and Dynamics of Polymers**

interaction	electronic structure	geometry	nuclei	structure	dynamics
chemical shift	yes	intrinsic and orientation	$^1\text{H}$ , $^{13}\text{C}$ , $^{15}\text{N}$ , $^{19}\text{F}$ , $^{29}\text{Si}$ , $^{31}\text{P}$	conformation, through-space proximities	conformational transitions, rotational motions
dipole–dipole coupling	no	internuclear distance and orientation	$^1\text{H}$ , $^{13}\text{C}$ , $^{15}\text{N}$ , $^{19}\text{F}$ , $^{29}\text{Si}$ , $^{31}\text{P}$	through-space distances	translational and rotational motions
<i>J</i> -coupling	yes	intrinsic, internuclear distance and orientation	$^1\text{H}$ , $^{13}\text{C}$ , $^{15}\text{N}$ , $^{19}\text{F}$ , $^{29}\text{Si}$ , $^{31}\text{P}$	conformation and intergroup binding	conformational transitions, rotational motions
quadrupole coupling	yes	intrinsic and orientation	$^2\text{H}$ , $^{14}\text{N}$ , $^{17}\text{O}$ , $^{23}\text{Na}$ , $^{27}\text{Al}$	symmetry of electronic environment, chemical bonding	rotational motions

**Table 2. Comparison of Scattering and NMR Techniques as Well as the Information Provided about Structure and Dynamics of Materials<sup>a</sup>**

		scattering		NMR	
		incoherent	coherent	single quantum	double quantum
dynamics	molecular	n-quasielastic	n-quasielastic	2D-, 3D-, 4D-exchange, pulsed field gradient	MAS-sidebands
structure	collective		n-spin-echo	2D-exchange	decay of DQC
	molecular		WAXS, WANS	chemical shift, MAS sidebands	2D pattern, MAS-sidebands
	collective (packing)		X-ray pole figures, SAXS, SANS	DECODER chemical shift	2D signal pattern

<sup>a</sup>WAXS: wide-angle X-ray scattering; SAXS: small-angle X-ray scattering; SANS: small-angle neutron scattering; MAS: magic angle spinning; DECODER: direction exchange with correlation for orientation–distribution evaluation and reconstruction; DQC: double quantum coherence.

oriented samples, e.g., fibers.<sup>8</sup> Again, remarkable advances in synchrotron X-ray sources<sup>30</sup> can be exploited in polymer physics, in particular for studying thin films.<sup>31</sup>

As scattering and NMR are both very versatile and can unravel the delicate interplay between structure and dynamics in complex soft matter systems, it is worthwhile to compare the two techniques in detail as done in Table 2.

**Other Techniques.** Scattering and NMR are by no means the only techniques to probe the interplay between structure and dynamics of macromolecular and supramolecular systems.

- Remarkable improvements have been achieved in broadband *dielectric spectroscopy* (DS). Today it routinely covers 10 orders of magnitude with highly improved sensitivity, such that weak dipoles and/or low amplitude motions can be elucidated<sup>32</sup> and dynamics in thin films are accessible.<sup>33</sup>

- Likewise, *electron paramagnetic resonance* (EPR) *spectroscopy*<sup>34</sup> of spin labels and spin probes in polymers enjoys a remarkable revival due to improved microwave technology, which now allows routine applications of pulsed EPR methods and high-field EPR with similar improvements as in high-field NMR. These techniques offer, e.g., easy access to probe counterion structure and dynamics in polyelectrolyte solutions.<sup>35</sup>

- *Optics* combined with *microscopy* also allows us to study structure and dynamics with unprecedented possibilities. In both cases, dye molecules are often used as tracers. As an example, translational diffusion of fluorescent tracers in various environments can be studied with very high sensitivity by fluorescence correlation spectroscopy (FCS). The method, originally developed for studying the diffusion of biomacromolecules, is based on detecting the fluctuations of the fluorescent light intensity caused by the diffusion through a small observation volume on the micrometer scale, formed by the focus of a confocal microscope.<sup>36</sup> Near-field techniques and low temperatures allow for observation at the single molecule level, which offers unique opportunities to unravel structure and dynamics of supramolecular structures of interest in photophysics.<sup>37</sup>

- For the improvement of processing polymer materials, their flow behavior is of utmost importance.<sup>38</sup> Here the recent development of *Fourier transform rheology*<sup>39</sup> is particularly important, as it offers a way to quantify nonlinear

flow of bulk polymers or polymer dispersions in a unique and quantitative way. For the latter, nonlinearity originating from strain hardening, strain softening, and wall slip could clearly be unraveled.<sup>40</sup>

This collection is certainly not complete but rather indicates the enormous improvement of characterization techniques achieved during the past decade or so.

## Examples

In a recent Perspective,<sup>10</sup> leading scientists in the polymer field have identified challenges and opportunities for research in macromolecular science. They point out that “advances in synthetic techniques and in polymer functionality both require and inspire advances in our ability to characterize molecular and material structure in detail.” The following examples have been selected bearing in mind this statement and some of the specific challenges mentioned in this paper.

**Morphology: Chain Organization and Mobility in Semicrystalline Polymers and Its Relation to Drawability.** The new NMR techniques provide new insight into one of the classics in polymer physics, namely the changes in mobility of chains in samples of different morphology.<sup>41</sup> In particular, the conformation of the chains at the interface between crystalline and noncrystalline regions in semicrystalline polymers is crucial for their dynamics. This was studied in ultrahigh molar mass linear polyethylene in the solid state comparing the behavior of solution crystallized (SC) and melt crystallized (MC) samples (Figure 2).<sup>42</sup> As expected, the higher conformational order in the SC samples leads to a significantly reduced local mobility as probed via  $^1\text{H}$ – $^{13}\text{C}$  dipole–dipole couplings compared with the MC sample. In contrast, chain diffusion is considerably faster in the SC samples, where on a much longer time scale the all-trans stems in the crystals diffuse to the gauche-containing noncrystalline regions and vice versa. Thus, extended conformations in the interphase between crystalline and noncrystalline regions of SC samples apparently facilitate chain diffusion (see Figure 2). The temperature dependence of the diffusive motion is similar in SC and MC samples. Therefore, the difference in time scale results from the entropy difference between SC and MC systems. Our conjecture is further supported by a recent study of



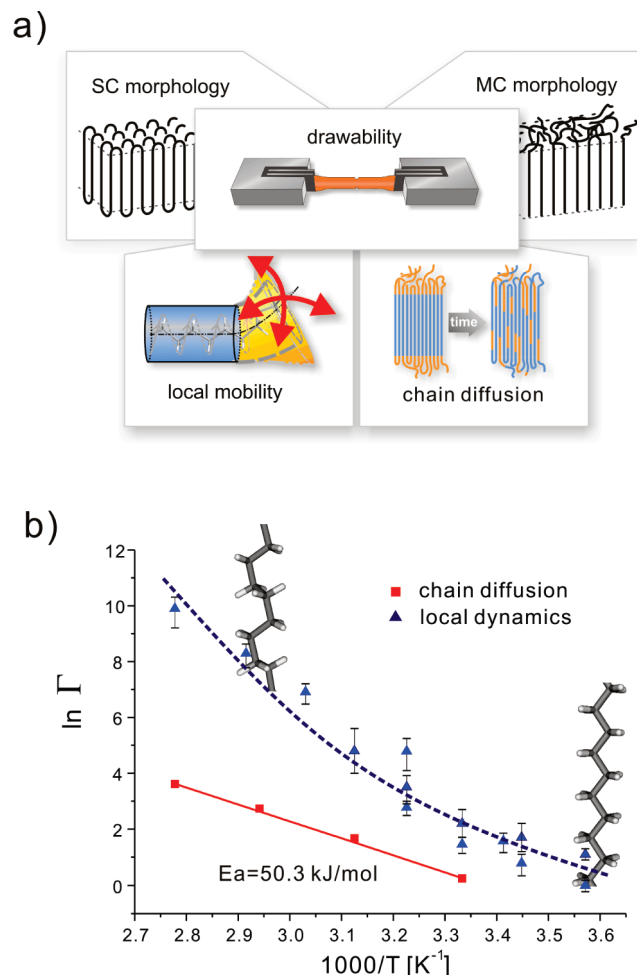


**Figure 2.** (a) Chain organization and chain motion in semicrystalline polyethylene. (b) Chain diffusion vs local jump rate of melt crystallized polyethylene. The former shows a simple Arrhenius behavior, whereas the latter display a pronounced curvature.

chain diffusion in monodisperse long *n*-alkanes<sup>43</sup> where it was found that the alkane chains can rapidly slide around a well-defined fold, while the chain-end methyl groups are constrained at the opposite lamella surface.

The comparison of the diffusion constant for the chain diffusion and for the local motion in the crystallites, also available from NMR, is even more interesting. Substantial acceleration of the local mobility with increasing temperature, as compared to the chain diffusion, is observed (Figure 2b), which can be attributed to the formation of defects in the expanded lattice. Contrary to textbook knowledge,<sup>41</sup> however, these defects are not effective in moving the whole stem, despite the fact that their mobility is detected by mechanical relaxation. Instead, twist modes of the entire stem, as discussed by Mansfield and Boyd in 1978 already,<sup>44</sup> are apparently able to drive chain diffusion.

Based on NMR observations of chain motion in polymer crystals, the crucial importance of chain diffusion for cold drawing of such polymers has been pointed out by Schmidt-Rohr.<sup>45</sup> Eventually, however, topological constraints (entanglements) in the noncrystalline regions limit the drawability.<sup>46</sup> By controlled synthesis the number of entanglements can be reduced. Ultimately, crystals composed of single chains are feasible, where the chains are fully separated from each other. As shown recently by a combination of rheology and NMR spectroscopy,<sup>47</sup> such separation can be maintained in the melt leading to a new "heterogeneous" melt with more entangled regions,

where the chains are mixed, and less entangled regions, composed of individually separated chains. On a molecular level, these differences in the melt structure were detected by a slight difference in chain dynamics via NMR spectroscopy. The long-lived heterogeneous melt shows decreased melt viscosity and indeed exhibits enhanced drawability on crystallization.

**Defects and Chain Branching.** The macroscopic properties of polyolefins strongly depend on the chain microstructure. In recent years new single site catalysts have enabled much greater synthetic control over the polydispersity, type of branch, and branch content.<sup>48</sup> In polyethylene, the physical properties of both the solid and the melt can be tuned by the presence of branches of various lengths in the polymer backbone. Such branches form structural defects during crystallization and thus strongly affect crystallization rates, crystallinity, and other bulk mechanical properties. For instance, long-chain branching is known to influence the zero-shear viscosity even at concentrations of 2 branches per 100 000  $\text{CH}_2$  groups. Thus, it is very important to quantify the degree of chain branching, and  $^{13}\text{C}$  NMR in solution seems to be the method of choice as the chemical shifts of branch points as well as adjacent carbon positions can be distinguished from the backbone resonances. However, when applied to polyethylene, exceedingly long measurement times are needed because of the low solubility of polyethylene, even at high temperatures. Solid state type NMR, under magic-angle spinning (MAS), on the other hand, can be used to overcome these limitations,<sup>49</sup> despite the substantial loss of spectral resolution as compared to solution NMR. Under optimized conditions about 2 orders of magnitude reduction of measuring times were achieved, allowing quantification of a few branches in 100 000  $\text{CH}_2$  groups in a single overnight run (see Figure 3a). Remarkably, the characterization of branch lengths up to 16 carbons in melt-state NMR is achieved by measuring relaxation times, i.e., discriminating the branches via their *dynamics* rather than by their chemical shift, based on the chemical *structure*.

Melt-state MAS NMR can also be used to study chain ends. This is particularly important to prove the cyclic nature of polymers generated by ring-expansion metathesis polymerization.<sup>50</sup> Cyclic polymers have been a fascinating macromolecular architecture for synthetic chemists as well as materials scientists and physicists ever since the discovery of circular DNA.<sup>51</sup> Constraining a macromolecule into a cyclic topology can result in unique properties in comparison with linear analogues such as lower viscosities, smaller hydrodynamic radii, and increased functional group density. Furthermore, cyclic polymers may challenge and expand fundamental knowledge regarding polymer properties as they relate to the presence and absence of chain ends. In view of the synthetic challenge producing this topology, being able to determine the absence of chain ends is particularly important.

In commercial polymer samples the irregular distribution of the branching sites along the main chain results in uncertainty of the branching influence on morphology, chain dynamics, and other physical properties. Here polyethylene samples with regularly spaced methyl branches obtained by acyclic diene metathesis (ADMET) polycondensation<sup>52</sup> provide much more specific information. By deuteration of the methyl branches, the molecular dynamics of the defect site can be studied selectively via  $^2\text{H}$  NMR, whereas molecular reorientations of the polymer chain between the branching sites can be monitored separately via  $^{13}\text{C}$  chemical shift anisotropy. Combining these results with studies of local conformations, a twist motion can be identified, which is centered at the branching sites for a spacing of about 20  $\text{CH}_2$  units between subsequent branching points. In methyl

branched PE samples with shorter spacing, e.g., 14 CH<sub>2</sub> units between subsequent methyl branches, a collective dynamic process emerges from this twist motion, which ultimately leads

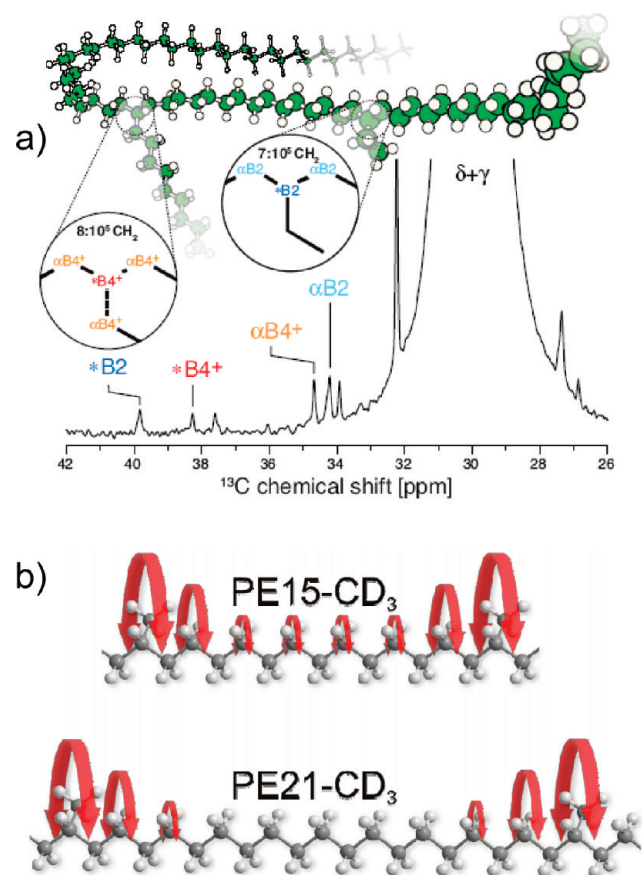


**Figure 3.** (a) Quantification of low branch content in optimized melt-state <sup>13</sup>C NMR under MAS; for details see ref 49. (b) Local and collective motions in precise polyethylene with CD<sub>3</sub> branches spaced every 15th and every 21st CH<sub>2</sub> group, PE15-CD<sub>3</sub> and PE21-CD<sub>3</sub>, respectively.

to the formation of a rotator phase as indicated in Figure 3b. Thus, localized and collective mobility induced by the defects can clearly be distinguished. The superb spectral resolution of a 850 MHz solid state NMR spectrometer was essential for obtaining these results.<sup>53</sup> It is rewarding to observe that chain twists considered above to be responsible for chain diffusion are actually found in this study of well-defined structure.

**Dynamic Heterogeneities at the Glass Transition and in the Glassy State.** Heterogeneity in structure and dynamics is a particularly characteristic feature of amorphous polymers. In the context of interplay of structure and dynamics, it can probably best be probed in polymer melts in the vicinity of the glass transition. Here, multidimensional exchange NMR<sup>8</sup> can provide information that was completely inaccessible before. As the geometry and the time scale of molecular motion are probed separately and, moreover, the motional behavior can be probed at up to four subsequent times, questions can be tackled such as *is the probability of undergoing a jump different after the group has performed a jump?* In a series of pioneering papers,<sup>54</sup> the nature of nonexponential relaxation in polymers in the vicinity of the glass transition was examined. This led to the concepts of *rate memory* and *dynamic heterogeneities*, which today are recognized as a signature of fragile glass-formers<sup>55,56</sup> (see Figure 4). The unique capabilities of NMR were exploited to develop a technique combining 4D-NMR with spin diffusion<sup>8</sup> that allowed us to detect not only the time scale of such heterogeneities but also their length scale in the nanometer range. It was found that the number of statistically independent units engaged in these heterogeneities is below 100. Therefore, it is tempting to relate them to the “cooperatively rearranging” units first postulated by Adam and Gibbs.<sup>57</sup> Indeed, computer simulations<sup>58</sup> show that such heterogeneities can even occur in simple hard-sphere systems as displayed in Figure 4c.

In physics terms the NMR techniques developed in the 1990s to elucidate dynamic heterogeneities provide *higher order correlation functions*.<sup>54,55,59</sup> The X-ray lasers currently being built several places are considered to provide excess to such functions in the future as well. Moreover, such dynamic heterogeneities can nowadays even be probed at the single

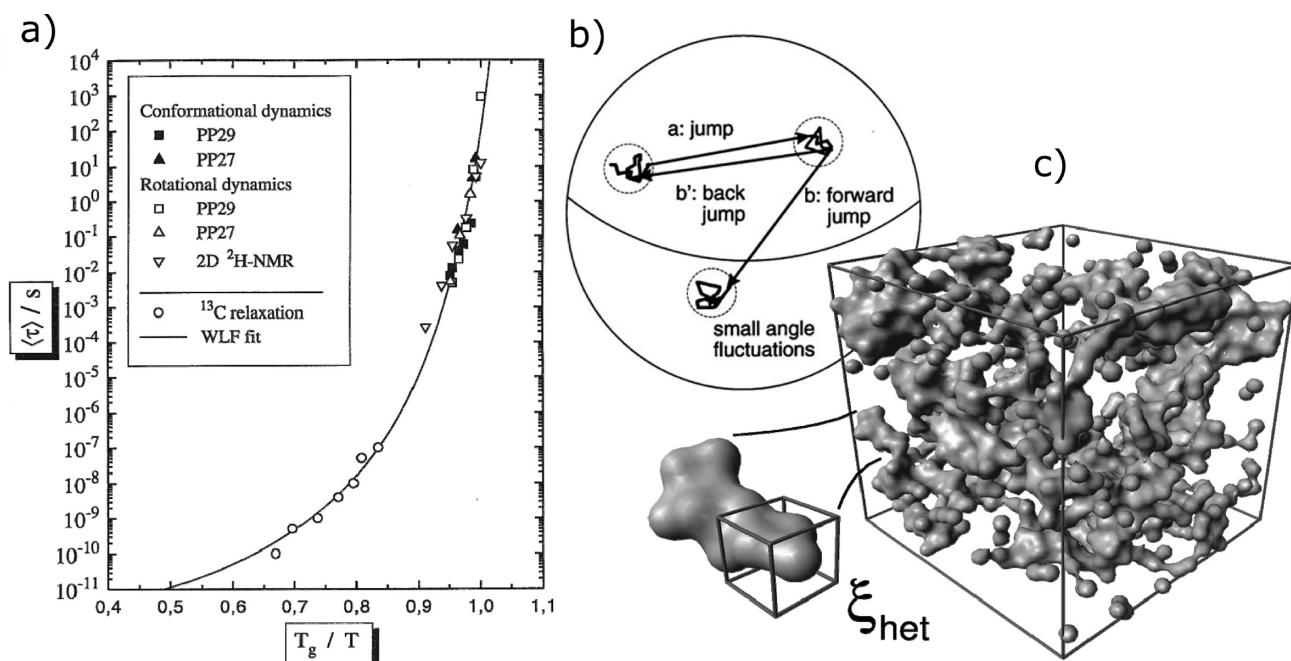


**Figure 4.** Complex dynamics at the glass transition of soft matter from multidimensional NMR: (a) correlation times of chain motion of atactic poly(propylene) from different NMR experiments; (b) geometry of rotational motions; (c) dynamic heterogeneities as visualized by computer simulation.

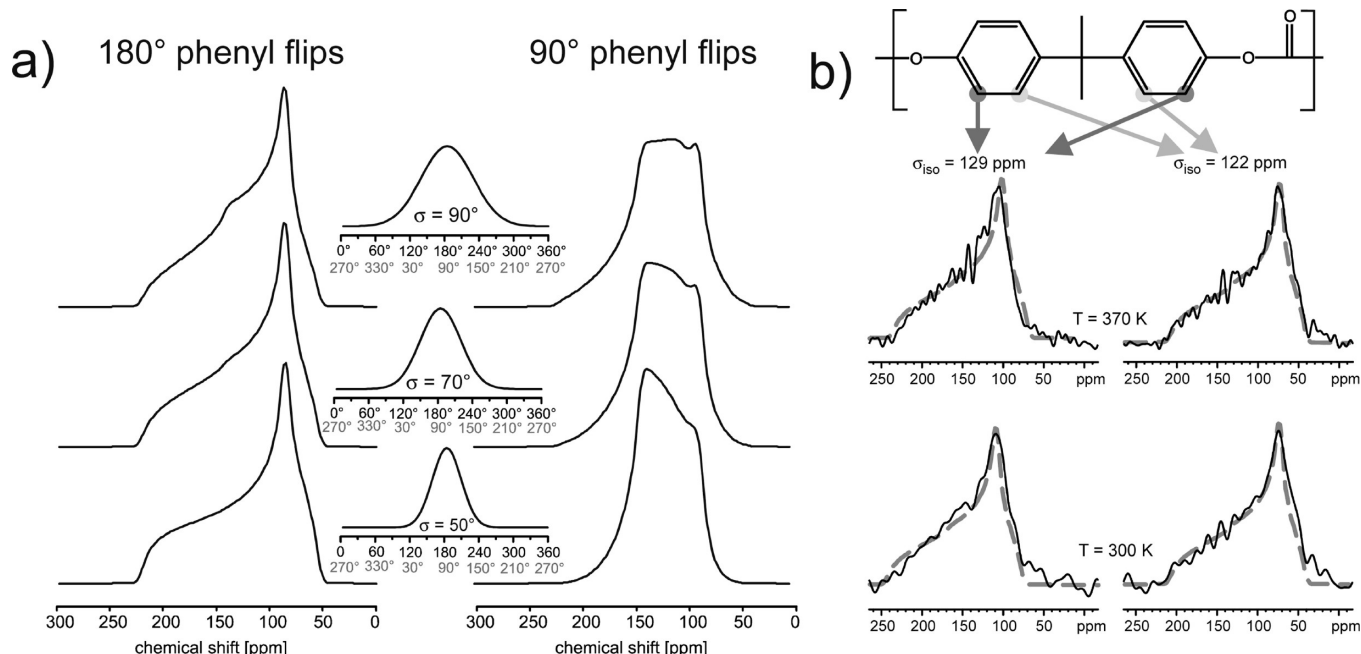


**Figure 5.** Heterogeneous phenylene dynamics in poly(carbonate).<sup>67</sup> (a) Line shape simulations for motionally narrowed  $^{13}\text{C}$  NMR spectra for heterogeneous Gaussian distributions of flip angles centered at 180° and 90° with different standard deviations  $\sigma$  as indicated. (b) Experimental  $^{13}\text{C}$  NMR spectra for the two distinct phenylene carbon positions in PC fitted to a heterogeneous Gaussian distribution with full width at half-maximum of 80° of flip angles centered at 180°, dashed line.

molecule level,<sup>60</sup> and the above conclusions are confirmed quantitatively.

Heterogeneities, however, not only concern the *time scale* of the molecular motion, they also apply to their *amplitude*. As far as sub- $T_g$  dynamics and its relation to ductility is concerned, bisphenol A polycarbonate (PC) is one of the most studied, yet still controversial, systems. For a recent review of the field see ref 61. From  $^2\text{H}$  NMR line shapes, large angle phenylene rotations described by 180° flips augmented by additional oscillations were identified at room temperature and above.<sup>62</sup> Such 180° flips were subsequently confirmed by  $^{13}\text{C}$  NMR line shape studies<sup>63</sup> and  $^2\text{H}$  2D exchange NMR at lower temperatures.<sup>64</sup> The time scale of the phenylene motion is in remarkable agreement with that of sub- $T_g$  mechanical relaxation. Under tensile stress, the time scale of the motion did not change significantly, but the heterogeneous Gaussian distribution of flip angles determined around 230 K broadened from 50° full width at half-maximum in PC without stress to 90° under 50 MPa tensile stress.<sup>64</sup> Thus, the phenylene motion seemed well characterized. Recently, the sub- $T_g$  dynamics of PC at ambient temperatures was also studied by quasielastic neutron scattering,<sup>65</sup> and it was concluded that in addition to ill-defined 180° flips the phenylene rings in PC exhibit a third motion, namely flips by 90° with correlation times in the range between 1 ns and 1 ps at temperatures of 300–400 K. This was inferred from an increase of the quasielastic scattering intensity above room temperature, which could not be accounted for by well-defined 180° flips alone. A full simulation of the scattering intensity considering a distribution of flip angles, however, was not attempted. With advanced 2D NMR techniques<sup>66</sup> probing the  $^{13}\text{C}$  anisotropic chemical shift, the geometry of the phenylene motion can be probed differently than via  $^2\text{H}$  quadrupole coupling, as the unique directions of the two interactions are mutually perpendicular. As seen in Figure 5a, 180° and 90° flips result in vastly different line shapes, yet the experimental spectra show no evidence of the latter. Instead, the phenylene motion in the glassy state displays a heterogeneous distribution of rotational angles, about 80° in width, centered at a flip angle

of 180°, which stays essentially constant over a wide temperature range.<sup>67</sup> Moreover, the presence of flip angles differing significantly from 180° readily explains the increase of quasielastic scattering intensity in the neutron data. The consistency of the results of the different NMR experiments and neutron scattering is truly gratifying. Moreover, the presence of flip angles significantly different from 180° provides a simple way of coupling the phenylene flips to other degrees of motion of the PC chain as well as mechanical relaxation. This is because the flip does not occur between equivalent positions of the group. Thus, the phenylene motion that can consistently be observed in NMR and neutron scattering experiments is sensitive to the details of the local packing.

It is interesting to note that distributions of fluctuation angles also occur in the dynamics of confined molecules in macroscopically oriented nanoporous systems<sup>68</sup> as observed by  $^2\text{H}$  solid-state NMR. Profound differences are found for guests in crystalline and noncrystalline polymers. In stretched crystalline polymer hosts, like the  $\delta$  phase of syndiotactic polystyrene, high orientation of the guest molecules can be achieved without changing their local environment. While the rotation axis can be fixed, large-amplitude motions can still occur, which is important information for tailoring *guest–host systems* for specific applications.<sup>69</sup>

**Heterogeneities in Functional Stimuli-Responsive Polymer Networks.** Polymer networks that can take up many times their own mass in water attract a lot of attention in materials science. Such networks can be chemically fine-tuned to expel water and collapse from a swollen state upon an external stimulus (temperature, pH, salt content, etc.).<sup>70,71</sup> This sensitivity toward external triggers makes polymer networks interesting for use as functional materials, e.g., in molecular sensors or as drug delivery agents. EPR spectroscopy of amphiphilic nitroxide spin probes offers an interesting way to study the release of small molecules. EPR spectroscopy on these reporter molecules shows high selectivity and site specificity and delivers a large variety of information on local guest–host interaction, the distribution of guest molecules (on the nanometer scale),



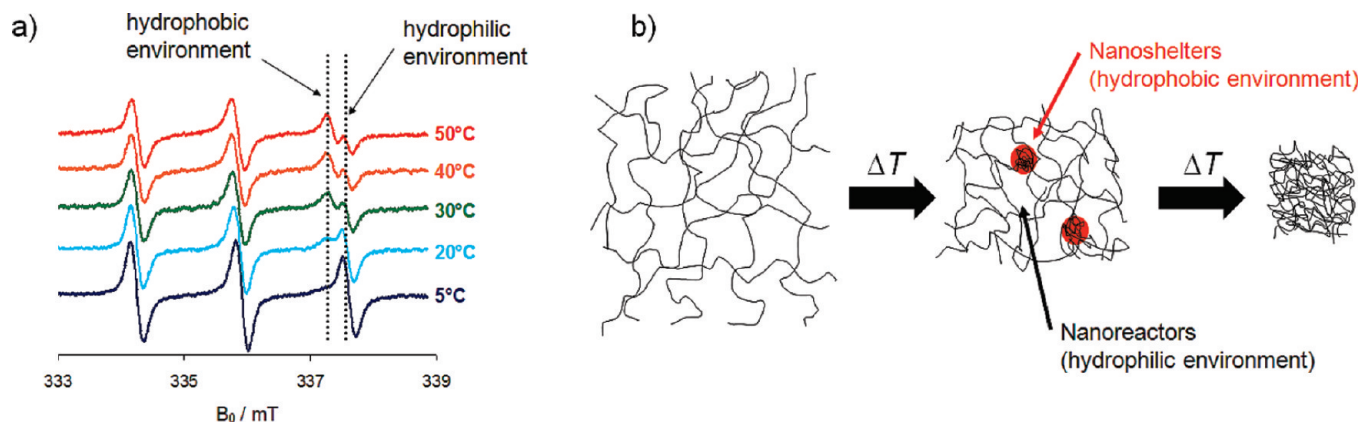


**Figure 6.** (a) Temperature-dependent CW EPR spectra of TEMPO in an aqueous solution with PNIPAAm-based hydrogels and comparison of TEMPO probes trapped in collapsed pockets and a macroscopic (AFM-based) observation of hydrogel collapse. (b) Model of network collapse as seen by EPR spin probes: individual pockets continuously collapse before the macroscopic collapse happens.

and accessibility by solvents. A recent study<sup>72</sup> along these lines on poly(*N*-isopropylacrylamide), PNIPAAm, revealed that small molecules are continuously released from the polymeric network when the temperature is increased (see Figure 6). However, macroscopically the polymeric network collapses rather sharply at the lower critical solution temperature (LCST) of the polymer, around 30 °C. These findings have led to the conclusion that the polymer network collapse is a continuous process, in which individual polymeric “pockets” are in a collapsed state even at temperatures significantly below the LCST and that the macroscopic collapse takes place only when a certain number and/or volume of collapsed “pockets” is reached. Remarkably, the hydrophilic regions form *nanoreactors*, which strongly accelerate acid-catalyzed disproportionation reactions while simultaneously the hydrophobic regions act as *nanoshelters*, in which enclosed spin probes are protected from the decay. The results show that the system consisting of a statistical binary or tertiary copolymer displays remarkably complex behavior that mimics spatial and chemical inhomogeneities observed in functional biopolymers such as enzymes.

Subsequently, a similar result of micro/nanophase separation was observed in block copolymers of PNIPAAm and *N*-isopropylmethacrylamide (PNIPMAM). This was concluded from small-angle neutron scattering (SANS) and analysis of the scattering with a new form factor model with a nanophase-separated internal morphology.<sup>73</sup> We note that the simple and cheap EPR method does not only *directly* mirror the nanophase separation in the CW EPR spectra without the use of any model, but even allows for the characterization of the nanoheterogeneity on the functional level of a chemical reaction.

Similarly, dendronized polymers, based on oligoethylene glycol (OEG) units, exhibit fast and fully reversible phase transitions due to dehydration of the more hydrophobic groups with a sharpness in turbidity measurements that is among the most extreme ever observed.<sup>74</sup> Their LCST is found in a physiologically interesting temperature regime between 30 and 36 °C. Probing the collapse on a molecular level with spin-label EPR spectroscopy as described above reveals, however, that the dehydration of the polymer chains proceeds over a temperature interval of at least 30 K. It cannot be described by a single deswelling process that would be expected for a thermodynamic phase transition. Rather, the dehydration should be viewed as a molecularly controlled nonequilibrium state and takes place in two steps. The local heterogeneities grow in size and polymer, chain fluctuations slow down. Within ~7 °C above  $T_C$ , the majority of the dehydration is completed, and percolation for the

fraction and volume of hydrophobic regions is reached. While the aggregation temperature mainly depends on the periphery of the dendrons, the dehydration process itself is sensitive to the inner core with the dehydration efficiency being strongly related to the core’s hydrophobicity.<sup>75</sup>

#### Translational Chain Motion in Entangled Polymer Melts.

Chain motion in entangled melts is a complex process involving many length and time scales.<sup>76</sup> A remarkable advance in understanding the processes involved was provided by the De Gennes reptation/tube model<sup>77</sup> (see Figure 7). Depending on the molecular weight of the chains and thus the number of entanglements per chain, the time scale of correlation loss associated with this process is more or less separated from the more localized Rouse modes, regimes I–II. In highly entangled melts the time scale for reptation between the longest constrained Rouse mode and the tube disengagement time ranges from about 0.1 ms up to seconds.<sup>78</sup> The simple fixed-tube model is insufficient for a quantitative description of rheological data, and ongoing discussions focus on including dynamics of the tube itself, caused by contour-length fluctuations arising from chain-end motions of the test chain, or constraint release, arising from matrix chain motions.<sup>79</sup> Microscopic, atomic-scale experiments focusing on the Doi–Edwards regimes II–IV (constrained Rouse, reptation, and terminal diffusion) can crucially test the fundamental model assumptions.<sup>80</sup>

Among the experimental techniques, neutron scattering<sup>22</sup> and NMR spectroscopy<sup>8</sup> are particularly informative because they are able to provide information on time scale *and* geometry of the motions. Thus, many studies aimed at checking the predictions of the tube model have been performed.<sup>19,28</sup> For high molar mass samples, however, reptation is outside the typical time window of neutron scattering. Thus, neutron scattering and diffusion NMR<sup>81</sup> are particularly suited to study regimes I and II in Figure 7. Advanced NMR techniques such as studying residual dipole–dipole couplings via double quantum coherences<sup>18–20</sup> are better suited to directly probe the slow dynamics in regime III and even IV. These NMR techniques provide access to the orientation autocorrelation function  $C(t)$  introduced by Ball, Callaghan, and Samulski,<sup>82</sup> which was measured directly in the time domain and applied to study reptation by Graf et al.<sup>83</sup> For a review and more recent studies, see ref 19. Moreover, NMR longitudinal relaxation at low fields offers another way to reach the necessary low frequencies and has successfully been applied to elucidate reptation dynamics.<sup>84</sup>

Recently, by combining these two NMR techniques, it was possible to monitor the dynamics of well-entangled polymer chains in the bulk melt over 10 orders of magnitude in time,

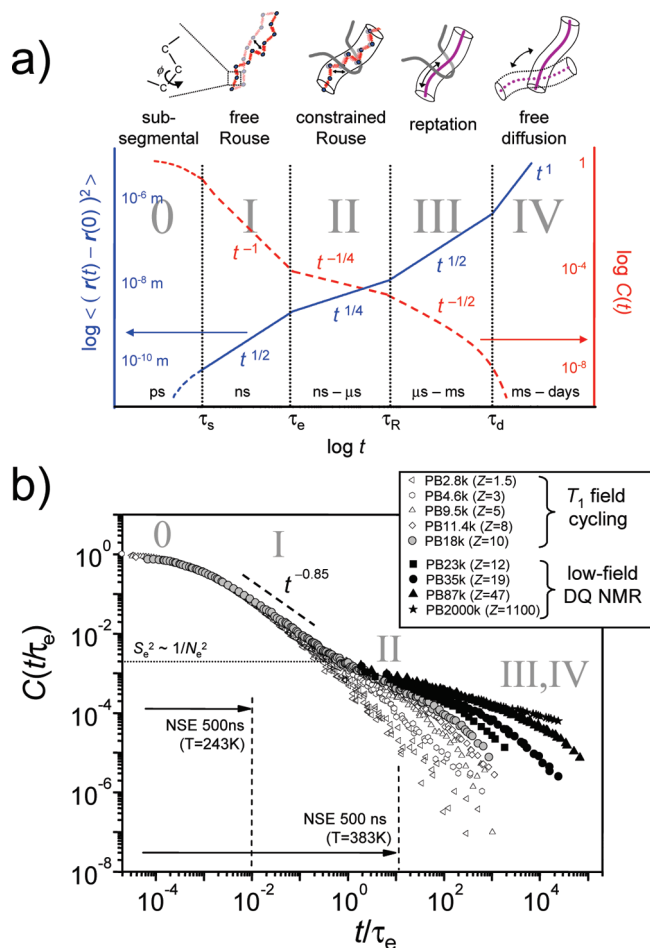


**Figure 7.** (a) Sketch of time and length scales for mean-square displacements  $\langle r(t) - r(0) \rangle$  of a segment of an entangled polymer chain, adapted from ref 76, and the orientation autocorrelation function,  $C(t)$ .<sup>19,82</sup> (b) Selected correlation functions  $C(t/\tau_e)$  for polybutadiene from double-quantum (DQ) NMR,<sup>85</sup> combined with  $T_1$  field-cycling NMR data from ref 84 covering the lower time range, with no relative shifts applied. The dashed lines indicate the approximate time limit for complementary NSE spectroscopy in the studied temperature interval.

covering the regimes II–IV of the tube model.<sup>84,85</sup> The familiar molar mass scaling of the Rouse and the disentanglement times was confirmed, but a characteristic variation of the scaling exponent describing the time dependence of segmental fluctuations in the constrained-Rouse regime II up to high molecular weights was observed. The local relaxation of well-entangled chains is thus governed by Rouse modes that are much less restricted than predicted by the tube model. Furthermore, by mixing chains of different molar mass and making one species unobservable via deuterium labeling, it was shown<sup>85</sup> that the scaling exponent is determined by the matrix chains alone, suggesting that constraint-release effects are responsible for the observed behavior (see Figure 7).

**Self-Assembly and Dynamics of Polypeptides.** Polypeptides (macromolecules composed of amino acids) play a vital part of the molecules designed for use in drug delivery or gene therapy and thus have been the subject of intensive studies.<sup>86,87</sup> These copolymers are produced commercially on an industrial scale by using conventional  $\alpha$ -amino acid *N*-carboxyanhydrides (NCA) ring-opening polymerization techniques. In addition, it is known that the superb performance of biological polypeptide-based materials such as hair or spiders' silk is due to a hierarchical superstructure with several length scales where structure control is exerted at every level of hierarchy. Their two most common

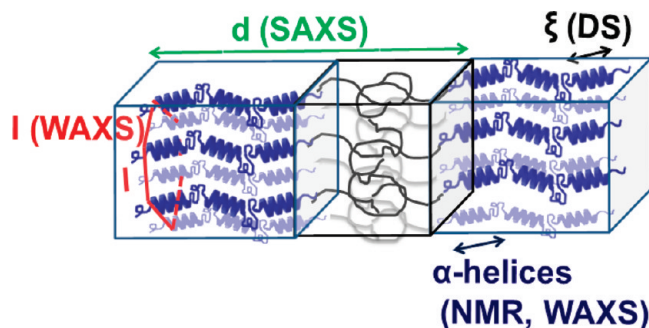


**Figure 8.** Assembly of a lamellae forming polypeptide-coil diblock copolymer depicting the main techniques employed to study their structure and dynamics small- and wide-angle X-ray scattering (SAXS, WAXS),  $^{13}\text{C}$  NMR, and dielectric spectroscopy (DS).

local conformations, known as secondary structures, are the  $\alpha$ -helix, stabilized by intramolecular hydrogen bonds, and the  $\beta$ -sheet, stabilized by intermolecular bonds. These secondary structures can be probed directly by solid state NMR,<sup>88</sup> and their packing can be obtained by X-rays. In addition, the  $\alpha$ -helical structure posts a permanent dipole moment along its backbone and can be, therefore, classified as type A polymer in Stockmayer's classification.<sup>32</sup> This dipole moment can be measured precisely using dielectric spectroscopy (DS) and can be used as a probe of the persistence length of the secondary structure, which is difficult to obtain by other methods.

Despite recent progress both in the synthesis<sup>87,89</sup> as well as in understanding the interplay between structure and dynamics of polypeptides (and proteins), several unresolved issues remain. These include<sup>90</sup> (i) the origin of a dynamic arrest at a "glass transition" temperature, i.e., at a temperature where the internal dynamics are practically frozen and the proteins are thus unable to function, (ii) the persistence length of  $\alpha$ -helices, and (iii) the effect of chain topology on the type and persistence of secondary structures. The complex self-assembly and the dynamics on different length and time scales require the use of a variety of powerful characterization techniques such as X-ray scattering, NMR, and dielectric spectroscopy (DS), see Figure 8. It depicts a lamellae forming polypeptide-*b*-coil diblock copolymer. Small-angle X-ray scattering (SAXS) is employed for the nano-domain spacing,  $d$ .  $^{13}\text{C}$  NMR and wide-angle X-ray scattering (WAXS) are employed to identify the type of the peptide secondary structure ( $\alpha$ -helical in Figure 8). WAXS is further employed to extract the lateral self-assembly of  $\alpha$ -helices within the polypeptide domain (a hexagonal lattice is indicated in the schematic). Dielectric spectroscopy and site-specific NMR techniques are employed to study the dynamics.

For example, *copolypeptides*, with their inherent nanometer length scale of phase separation, provide the means of manipulating both the type and persistence of peptide secondary structures. Specifically, partial annihilation of  $\alpha$ -helical structural defects due to chain stretching, induced chain folding of  $\beta$ -sheets in block copolypeptides with incommensurate dimensions, and destabilization of  $\beta$ -sheets in peptidic blocks having both secondary motifs were identified.<sup>91</sup> These effects should be taken into account when such peptides are considered for drug delivery. Polypeptide *star polymers* with a large hydrocarbon core were found to have several unanticipated properties.<sup>92</sup> First, with the aid of a polyphenylene core scaffold it was shown that there is a distinct change in the peptide secondary structure from coil/ $\beta$ -sheet conformations to  $\alpha$ -helices accompanied by an abrupt increase in the hydrodynamic radii. This change in secondary structure and the consequences on the particles' diffusion, measured by confocal fluorescence correlation



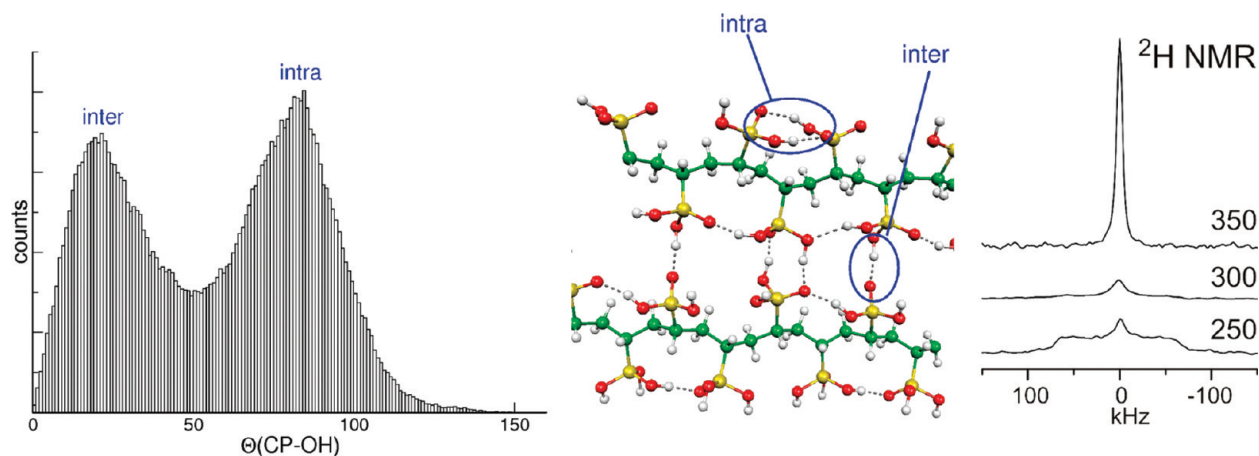


**Figure 9.** Left: distribution of the CP–OH angle within a given phosphonic acid group of poly(vinylphosphonic acid) PVPA, predicted from first-principles molecular dynamics simulations. Right: experimental  $^2\text{H}$  NMR line shapes as a function of temperature, illustrating motional narrowing due to the hydrogen bond dynamics, exhibiting an effectively isotropic motion.

spectroscopy, can be crucial in the efficient design of multiple antigen peptides. Second, the bulk studies revealed a strong effect of the polyphenylene core on the peptide secondary motifs that could not be envisaged from their linear analogues. Clearly, the local conformation of the peptides is a key parameter for understanding these systems, and the concerted use of the different techniques provides considerable more information than using either one alone.<sup>90</sup>

**Interplay of Structure and Dynamics in Polymeric Proton Conductors.** The growing necessity for clean energy sources to substitute fossil energy has created high demands for batteries and fuel cells. Therefore, various approaches have been proposed aiming at developing new classes of proton conducting membranes for high temperature applications.<sup>93</sup> Nafion, the most widely used membrane material, is a perfluorinated polymer that stands out for its high, selective permeability to water and small cations, in particular protons. The chemical structure of Nafion combines a hydrophobic Teflon-like backbone with hydrophilic ionic side groups.<sup>94</sup> Despite its technological importance, the structure of the Nafion ionomer used in proton-exchange membranes of  $\text{H}_2/\text{O}_2$  fuel cells has long been contentious. Recently an advanced analysis of small-angle X-ray scattering data of hydrated Nafion was performed by calculating the SAXS curve by a numerical Fourier transform from a given scattering density distribution.<sup>95</sup> In a thorough study combining solid state NMR with this new analysis of the SAXS curve it was concluded that the characteristic “ionomer peak” arises from long parallel but otherwise randomly packed water channels. These channels are surrounded by partially hydrophilic side branches, forming inverted-micelle cylinders.<sup>96</sup> At 20 vol % water, the water channels have an average diameter of 2.4 nm. The new model can explain important features of Nafion, including fast diffusion of water and protons through Nafion and its persistence at low temperatures.

For technical reasons such as methanol crossover and CO poisoning of the electrodes, a high temperature operation ( $T > 100^\circ\text{C}$ ) of fuel cells would be favorable. However, proton conduction drops dramatically in Nafion and related membranes when the proton carrying liquid water evaporates from the membrane. Therefore, proton transport membranes are desired, which do not rely on the diffusion of small proton carrying molecules (vehicle mechanism) and can efficiently operate at temperatures above  $100^\circ\text{C}$ . In fact, such materials are considered to be one of the keys to further progress in PEM fuel cell technology.<sup>93</sup> One promising approach in the development of

such a material is to combine the functions of the protogenic group and the proton solvent in a single molecule. Such molecules must be amphoteric in the sense that they behave as both a proton donor (acid) and proton acceptor (base), and they must form dynamical hydrogen bond networks. The first leads to the formation of a high concentration of intrinsic protonic defects as a result of self-dissociation, and the latter may promote a high mobility of these protonic charge carriers (excess and deficient protons). It should be noted that the mobility of intrinsic defects is generally higher than that of extrinsic defects, which may be introduced by acid or basic doping disturbing the local symmetry of the hydrogen bond network.

Typical amphoteric liquids include phosphoric acid and diverse heterocycles such as imidazole, pyrazole, benzimidazole, and triazole. In the liquid state, they all show relatively high proton conductivities with significant contributions from structure diffusion, i.e., the motion of protonic defects (excess or deficient protons) via intermolecular proton transfer, coupled to hydrogen bond breaking and forming processes.<sup>93</sup> A promising approach to eliminate the liquid electrolyte is to attach the protic groups of the liquid electrolyte to the backbone of the polymer, such that only chemical decomposition would result in a loss of ion carriers, a prominent example being poly(vinylphosphonic acid).<sup>97</sup> From  $^1\text{H}$ ,  $^2\text{H}$ ,  $^{13}\text{C}$ , and  $^{31}\text{P}$  NMR combined with computer simulation, detailed information on the proton mobility, water content, and the unwanted condensation of the phosphonic acid groups can be obtained. High mobility is found for the protons, whereas on the same time scale no mobility associated with reorientation of the phosphonic acid groups or the polymer backbone is observed. The  $^1\text{H}$  chemical shifts of P–OH protons provide evidence for the presence of a complex hydrogen bond network (see Figure 9), which allows for proton transport via a Grotthus-type mechanism along a given chain as well as between adjacent chains. The MD simulations further show that proton vacancies can be trapped in the anhydride defect produced by the condensation. More important, as shown in Figure 9 the highest intrinsic proton mobility arises in systems like poly(vinylphosphonic acids) where the hydrogen-bonded network is highly *disordered*,<sup>98</sup> characteristic of a hopping mechanism for proton conductivity.

In systems where the hydrogen-bonding network is separated from the polymer backbone via a spacer, a concept well-established in both synthetic and biological functional systems, site-selective NMR provides unique information about the interplay between local structure and the dynamics of the units involved and proton mobility. In the case of a

triazole functional polysiloxane, both the thermodynamics and the kinetics of formation and breaking of the hydrogen bonds could be followed by NMR.<sup>99</sup> This reveals that molecular reorientations of the triazole ring are essential for the proton transport. However, all activation energies of the microscopic processes are lower than that of the proton conductivity itself, indicating that there is an additional energy barrier controlling the macroscopic proton transport. This is not monitored in the local processes observed by NMR. Similar behavior is observed in phosphonic acid-based systems.

Last but not least, different protogenic groups can be mixed in one system, e.g., by attaching them to the same or different polymer chains. Along these lines imidazole methylphosphonate models have been investigated to elucidate hydrogen bonding and dynamics of a potential anhydrous polymer electrolyte.<sup>100</sup> This model salt exhibits ionic conductivity in the solid state, and the way of ion conduction in the solid state differs depending on the choice of anion and cation pairs. Increasing temperature introduces thermal motion and promotes the rotation of the imidazole ring together with the rotation of the phosphonate group. This leads to a cooperative mechanism of ion conduction between imidazole and the methylphosphonate at higher temperatures, which was unseen in a previous study of the benzimidazole methylphosphonate analogue.<sup>101</sup>

**Interplay of Structure and Dynamics in Columnar Structures for Organic Electronics.** Research on soft matter today includes supramolecular assemblies beyond polymers with different architectures.<sup>10</sup> Discotic liquid crystals, consisting of rigid disk-shaped aromatic cores and disordered alkyl substituents are prominent examples as they are able to organize into columnar supramolecular structures. Their self-assembly is driven by the  $\pi$ - $\pi$  overlap of the disks and the unfavorable interactions between the cores and the alkyl chains that lead to nanoscale self-assemblies.<sup>102</sup> Applications of such systems as electronic devices rely on the optimal stacking of the aromatic cores that allow for charge carrier mobility along the columnar axis (i.e., molecular wires).<sup>103</sup> With this in mind, the self-assembly and electronic properties of large aryl cores such as hexa-*peri*-hexabenzocoronenes have been explored extensively.<sup>104</sup> Recently, pigments such as peryleneimide derivatives have gained attention because of the opportunities presented by the combination of their liquid-crystalline, photophysical, semiconducting, and photoconducting properties.<sup>102,105,106</sup> The degree of structural perfection strongly affects their molecular properties (absorbance, fluorescence, and charge transport) and results in applications in organic field-effect transistors, light-emitting diodes, and organic solar cells. The supramolecular organization can be improved by generating helical structures through the appropriate choice of side groups by attaching the disks to a helical polymer backbone or by the structure of the core itself.<sup>107,108</sup>

Molecular dynamics of these complex systems is the key to the processing and self-healing capabilities of such molecular assemblies.<sup>109</sup> Since many of the early systems are symmetric, they do not carry a dipole moment. Therefore, the use of dielectric spectroscopy is limited. The prominent dynamic process in discotics involves axial rotation of the disks around the column axis. This has been established by <sup>2</sup>H solid state type NMR on samples aligned in magnetic fields as early as 1981<sup>110</sup> and has meanwhile been confirmed by innumerable <sup>1</sup>H, <sup>2</sup>H, and <sup>13</sup>C NMR studies,<sup>5,20</sup> including a detailed elucidation of the rotational angles involved by two-dimensional exchange NMR.<sup>111</sup> This axial rotation happens on relatively long time scales, ranging from a few

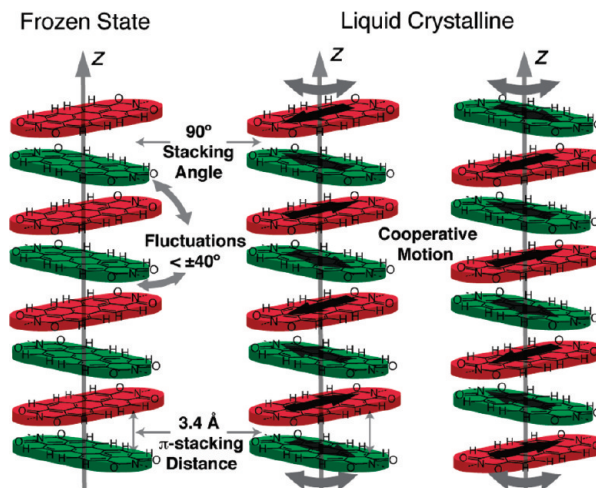


**Figure 10.** Scheme of axial motion for a perylene discotic in its two thermotropic phases. In the frozen state, in-plane local fluctuations of the cores occur independently. In the LC phase, a cooperative motion along the stacking axis cooperatively rotates the molecules by 90° in a spiral type of way.

hundred nanoseconds in the liquid-crystalline state to seconds in glass forming discotics, as proved from combining NMR with broad-band dielectric spectroscopy.<sup>112</sup> Notably, NMR not only detects the axial motion, it also provides information about the packing order within the column via the corresponding site selective order parameter. This order is typically very high in columns with small disks, in particular the triphenylenes,<sup>110,111</sup> while it can be significantly lower in the larger disks such as hexabenzocoronene (HBC).<sup>113</sup> Again, neutron scattering can provide detailed information on the dynamics on shorter time scales.<sup>114</sup> Small-angle fluctuations were identified, which can have important impact on the charge carrier mobility, which happens on similar time scales.<sup>115</sup> Thus, only the combination of the two techniques can provide the full picture.

In columns with a helical superstructure the rotation of the disks cannot occur as a simple local process but requires *cooperative motions* within the column in order to preserve the correlation between adjacent moieties. This was first demonstrated in a study combining dielectric spectroscopy and NMR on dipole functionalized HBCs, where two distinct modes were observed.<sup>116</sup> The faster mode is associated with local axial rotation of the disks with limited amplitude; the second one is ascribed to the cooperative complete axial rotation. In columns composed of perylene derivatives the pitch angle between adjacent moieties depends on a delicate balance of  $\pi$ - $\pi$  interaction and the organization of the side groups.<sup>117</sup> In a highly ordered system, where the perylene moieties are packed perpendicular to each other, local and cooperative motions could be nicely separated.<sup>118</sup> From a combination of various <sup>13</sup>C solid state NMR experiments local axial fluctuations of substantial amplitude were deduced in the solid, and full cooperative axial rotation was found in the liquid crystalline phase (see Figure 10). The cooperative dynamics in the liquid crystalline phase shows that indeed the correlation between adjacent perylene units is maintained during the axial rotation. Such cooperative dynamic modes are particularly important in processing columnar discotic systems to align on surfaces.

## Conclusions and Outlook

Advances in synthesizing, characterizing, and understanding macromolecular and supramolecular systems have led to an enormous variety and complexity in the field of polymer science.

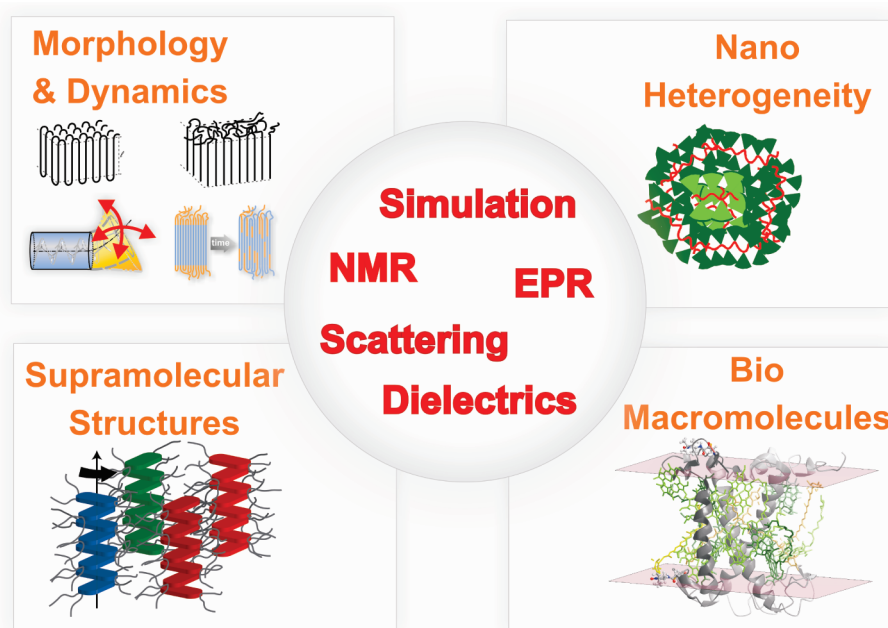


**Figure 11.** Overview of systems, phenomena, and techniques for elucidating the interplay between structure and dynamics in macromolecular and supramolecular systems.

The traditional separation in terms of structure vs dynamics, crystalline vs amorphous, or experiment vs theory is increasingly overcome. As far as characterization of such materials is concerned, no experimental or theoretical/simulation approach alone can provide full information. Instead, a combination of techniques is called for, and conclusions should be backed by results provided by as many complementary methods as possible. Combining scattering or NMR spectroscopy with computer simulation is well established today in the study of structure and dynamics of biomacromolecules.<sup>119</sup> Prominent pioneering examples of such an approach in the supramolecular field involved the combination of spectroscopy and computer simulation to elucidate the packing in columnar systems<sup>120</sup> and the proton conducting network in a new type of proton conductor.<sup>121</sup> Elucidating slow dynamics in this way is limited by the current capability of computers. The much faster motions accessible by neutron scattering or NMR relaxation can already be analyzed by computer simulation.<sup>122</sup> Advantage should be taken, however, of the fact that a general formalism exists, which does not involve the usual assumption of exponential relaxation and can handle locally anisotropic motion.<sup>123</sup> Indeed, in a recent *ab initio* calculation of  $^2\text{H}$  and  $^{17}\text{O}$  relaxation in water, without any empirical parameters or model assumptions a pleasing agreement with experimental data was found.<sup>124</sup> Remarkably, however, the simulated correlation function differs significantly from a simple exponential.

The examples described above, namely *morphology*, *defects*, *heterogeneities*, *local* and *collective dynamics*, and *biomacromolecules* and *hybrids*, are explicitly mentioned among the “challenges and opportunities” of research in macromolecular science.<sup>10</sup> They also reflect topics studied in our Institute, which celebrated its 25th anniversary last year.<sup>125</sup> These examples, although far from complete, also illustrate the special role of magnetic resonance techniques, in particular solid-state-type NMR, in elucidating the interplay between structure and dynamics in these systems (see Figure 11). Phase separation in polymer blends and block copolymers have been subjects of recent Perspectives<sup>126,127</sup> and will not be treated in detail here, but we point out that one- and two-dimensional NMR techniques allow selective determination of the glass transition via the time scales of slow chain dynamics for polymers in mixed systems relative to their pure

states<sup>128–130</sup> and the role of configurational entropy.<sup>131</sup> In case of biomacromolecules we, again, refer to a recent Perspective.<sup>132</sup> The role of NMR is well established in this area (see above). A particular intriguing question involving the interplay of structure and dynamics concerns the molecular processes leading to protein folding.<sup>133</sup> These processes can now be followed by pulsed double electron electron resonance (DEER).<sup>134</sup> This has recently been demonstrated by elucidating the refolding of the integral membrane protein light-harvesting complex II following the formation of different structural elements of the complex in real time.<sup>135</sup>

The development of NMR and pulsed EPR spectroscopy is far from complete. In particular, in order to meet the ever-increasing demands of miniaturization, the sensitivity of NMR spectroscopy has to be increased substantially, and several approaches to respond to that challenge are underway.<sup>136</sup> Moreover, studies of the activity of olefin metathesis catalysts by solid state NMR have shown how sophisticated multidimensional NMR techniques can be employed to fully characterize catalytic species on silica surfaces to obtain structural and dynamic parameters related to their reactivity.<sup>137</sup> Similarly, NMR methodology has been developed to monitor structural changes that occur during the operation of Li ion batteries.<sup>138</sup> These *in situ* NMR studies allow one, for example, to capture metastable phases, to follow reactions between the electrolyte and the electrode materials, and to investigate the effect of rapid charging and cycling of the battery.<sup>139</sup> Thus, in the future, it will be possible to elucidate the relation between structure, dynamics, and function by experiments on devices rather than materials, as is already the case in photophysics today.<sup>140,141</sup>

**Acknowledgment.** This paper is based on my working experience at the Max Planck Institute for Polymer Research for more than 25 years. It has provided me with a unique scientific environment, in which new ideas and approaches prospered. It gives me great pleasure to thank my colleagues and co-workers for all their contributions. Special thanks go to K. Saalwächter for providing ref 85 prior to publication as well as Figure 7 and to R. Graf, M. R. Hansen, D. Hinderberger, and S. Pinnells for carefully checking the manuscript.



## References and Notes

- (1) *Encyclopedia of Materials: Science and Technology*; Buschow, K. H. J., Calm, R. W., Flemings, M. C., Ilschner, B., Kramer, E. J., Mahajan, S., Eds.; Elsevier: Amsterdam, 2001.
- (2) *Macromolecular Engineering: Precise Synthesis, Materials Properties, Applications*; Matyjaszewski, K., Gnanou, Y., Leibler, L., Eds.; Wiley-VCH: Weinheim, 2007.
- (3) Lehn, J. M. *Science* **2002**, 295, 2400–2403.
- (4) Berne, B. J.; Pecora, R. *Dynamic Light Scattering*; Dover: Mineola, 2000.
- (5) *Handbook of Liquid Crystals*; Demus, D., Goodby, J., Gray, G. W., Spiess, H. W., Vill, V., Eds.; Wiley-VCH: Weinheim, 1998.
- (6) Kovacs, A. J. *J. Polym. Sci.* **1958**, 30, 131–147.
- (7) Wagner, H.; Richert, R. *Polymer* **1997**, 38, 255–261.
- (8) Schmidt-Rohr, K.; Spiess, H. W. *Multidimensional Solid-State NMR and Polymers*; Academic Press: New York, 1994.
- (9) Peter, C.; Kremer, K. *Soft Matter* **2009**, 5, 4357–4366.
- (10) Ober, C. K.; Cheng, S. Z. D.; Hammond, P. T.; Muthukumar, M.; Reichmanis, E.; Woolex, K. L.; Lodge, T. P. *Macromolecules* **2009**, 42, 465–471.
- (11) *Encyclopedia of Nuclear Magnetic Resonance*; Grant, D. M., Harris, R. K., Eds.; Wiley: Chichester, 1996.
- (12) Ernst, R. R.; Bodenhausen, G.; Wokaun, A. *Principles of Nuclear Magnetic Resonance in One and Two Dimensions*; Clarendon Press: Oxford, 1987.
- (13) Blümich, B. *NMR Imaging of Materials*; Clarendon Press: Oxford, 2000.
- (14) Munowitz, M.; Pines, A. *Adv. Chem. Phys.* **1987**, 66, 1–152.
- (15) Ward, I. M. *Structure and Properties of Oriented Polymers*; Chapman & Hall: London, 1997.
- (16) Wüthrich, K. *NMR of Proteins and Nucleic Acids*; Wiley: New York, 1986.
- (17) Al Amri, A.; Sahoo, S. K.; Monwar, M.; McCord, E. F.; Rinaldi, P. L. *Macromolecules* **2006**, 39, 5768–5776.
- (18) Spiess, H. W. *J. Polym. Sci.* **2004**, A 42, 5031–5044.
- (19) Saalwächter, K. *Prog. Nucl. Magn. Reson. Spectrosc.* **2007**, 51, 1–35.
- (20) Brown, S. P. *Macromol. Rapid Commun.* **2009**, 30, 688–716.
- (21) Warren, B. E. *X-Ray Diffraction*; Dover: Mineola, 1990.
- (22) Higgins, J. S.; Benoit, H. C. *Polymers and Neutron Scattering*; Oxford University Press: Oxford, 1997.
- (23) Fujara, F.; Wefing, S.; Spiess, H. W. *J. Chem. Phys.* **1986**, 84, 4579–4584.
- (24) Callaghan, P. T. *Principles of Nuclear Magnetic Resonance Microscopy*; Oxford University Press: Oxford, 1991.
- (25) Fleischer, G.; Fujara, F. *NMR: Basic Princ. Prog.* **1994**, 30, 159–207.
- (26) Scheler, U. *Curr. Opin. Colloid Interface Sci.* **2009**, 14, 212–215.
- (27) See <http://www.sns.gov/facilities/SNS/>.
- (28) Richter, D.; Monkenbusch, M.; Arbe, A.; Colmenero, J. *Adv. Polym. Sci.* **2005**, 174, 1–221.
- (29) Schmidt-Rohr, K.; Hehn, M.; Schaefer, D.; Spiess, H. W. *J. Chem. Phys.* **1992**, 97, 2247–2262.
- (30) Stribeck, N. *X-Ray Scattering of Soft Matter*; Springer: Heidelberg, 2007.
- (31) Müller-Buschbaum, P.; Wunnicke, O.; Stamm, M.; Lin, Y. C.; Müller, M. *Macromolecules* **2005**, 38, 3406–3413.
- (32) *Broadband Dielectric Spectroscopy*; Kremer, F., Schönhals, A., Eds.; Springer: Berlin, 2002.
- (33) Serghei, A.; Tress, M.; Kremer, F. *J. Chem. Phys.* **2009**, 131, 154904.
- (34) Schlick, S. *Advanced ESR Methods in Polymer Research*; Wiley-Interscience: Hoboken, NJ, 2006.
- (35) Hinderberger, D.; Spiess, H. W.; Jeschke, G. *Appl. Magn. Reson.* **2010**, 37, 657–683.
- (36) Walter, N. G.; Schwill, P.; Eigen, M. *Proc. Natl. Acad. Sci. U.S.A.* **1996**, 93, 12805–12810.
- (37) Wöll, D.; Braeken, E.; Deres, A.; De Schryver, F. C.; Uji-i, H.; Hofkens, J. *J. Chem. Soc. Rev.* **2009**, 38, 313–328.
- (38) Macosko, C. W. *Rheology: Principles, Measurements, and Applications*; Wiley-VCH: New York, 1994.
- (39) Wilhelm, M. *Macromol. Mater. Eng.* **2002**, 287, 83–105.
- (40) Klein, C. O.; Spiess, H. W.; Calin, A.; Balan, C.; Wilhelm, M. *Macromolecules* **2007**, 40, 4250–4259.
- (41) Stroh, G. *The Physics of Polymers*; Springer-Verlag: Berlin, 1997.
- (42) (a) Yao, Y.-F.; Graf, R.; Spiess, H. W.; Rastogi, S.; Lippits, D. R. *Phys. Rev. E* **2007**, 76, 060801(R). (b) Yao, Y.-F.; Graf, R.; Spiess, H. W.; Rastogi, S. *Macromolecules* **2008**, 41, 2514–2519. (c) Yao, Y.-F.; Graf, R.; Spiess, H. W.; Rastogi, S. *Macromol. Rapid Commun.* **2009**, 30, 1123–1127.
- (43) Grasso, G.; Titman, J. J. *Macromolecules* **2009**, 42, 4175–4180.
- (44) Mansfield, M.; Boyd, R. H. *J. Polym. Sci., Part B: Polym. Phys.* **1978**, 16, 1227–1252.
- (45) Hu, W. G.; Schmidt-Rohr, K. *Acta Polym.* **1999**, 50, 271–285.
- (46) Smith, P.; Lemstra, P. J. *J. Mater. Sci.* **1980**, 15, 505–514.
- (47) Rastogi, S.; Lippits, D. R.; Peters, G. W. M.; Graf, R.; Yao, Y.; Spiess, H. W. *Nat. Mater.* **2005**, 4, 635–641.
- (48) Brintzinger, H. H.; Fischer, D.; Mülhaupt, R.; Rieger, B.; Waymouth, R. M. *Angew. Chem., Int. Ed.* **1995**, 34, 1143–1170.
- (49) (a) Klimke, K.; Parkinson, M.; Piel, C.; Kaminsky, W.; Spiess, H. W.; Wilhelm, M. *Macromol. Chem. Phys.* **2006**, 207, 382–395. (b) Parkinson, M.; Klimke, K.; Spiess, H. W.; Wilhelm, M. *Macromol. Chem. Phys.* **2007**, 208, 2128–2133.
- (50) Xia, Y.; Boydston, A. J.; Yao, Y. F.; Kornfield, J. A.; Gorodetskaya, I. A.; Spiess, H. W.; Grubbs, R. H. *J. Am. Chem. Soc.* **2009**, 131, 2670–2677.
- (51) Semlyen, J. A. *Cyclic Polymers*, 2nd ed.; Kluwer Academic Publishers: Boston, 2000.
- (52) Baughman, T. W.; Wagener, K. B. *Adv. Polym. Sci.* **2005**, 176, 1–42.
- (53) Wei, Y.; Graf, R.; Sworen, J. C.; Cheng, C. Y.; Bowers, C. R.; Wagener, K. B.; Spiess, H. W. *Angew. Chem., Int. Ed.* **2009**, 48, 4617–4620.
- (54) (a) Schmidt-Rohr, K.; Spiess, H. W. *Phys. Rev. Lett.* **1991**, 66, 3020–3023. (b) Heuer, A.; Wilhelm, M.; Zimmermann, H.; Spiess, H. W. *Phys. Rev. Lett.* **1995**, 75, 2851–2854. (c) Tracht, U.; Wilhelm, M.; Heuer, A.; Feng, H.; Schmidt-Rohr, K.; Spiess, H. W. *Phys. Rev. Lett.* **1998**, 81, 2727–2730.
- (55) Sillescu, H. *J. Non-Cryst. Solids* **1999**, 243, 81–108.
- (56) Ediger, M. D. *Annu. Rev. Phys. Chem.* **2000**, 51, 99–128.
- (57) Adam, G.; Gibbs, J. H. *J. Chem. Phys.* **1965**, 43, 139–146.
- (58) Reinsberg, S. A.; Heuer, A.; Doliwa, B.; Zimmermann, H.; Spiess, H. W. *J. Non-Cryst. Solids* **2002**, 307–310, 208–214.
- (59) Boehmer, R.; Diezemann, G.; Hinze, G.; Roessler, E. *Prog. Nucl. Magn. Reson. Spectrosc.* **2001**, 39, 191–267.
- (60) Deschenes, L. A.; Van den Bout, D. A. *J. Phys. Chem. B* **2002**, 106, 11438–11445.
- (61) Monnerie, L.; Lauprêtre, F.; Halary, J. L. *Adv. Polym. Sci.* **2005**, 187, 35–213.
- (62) Spiess, H. W. *Colloid Polym. Sci.* **1983**, 261, 193–209.
- (63) Roy, A. K.; Jones, A. A.; Inglefield, P. *Macromolecules* **1986**, 19, 1356–1362.
- (64) Hansen, M. T.; Blümich, B.; Boeffel, C.; Spiess, H. W.; Morbitzer, L.; Zembrod, A. *Macromolecules* **1992**, 25, 5542–5544.
- (65) Arrese-Igor, S.; Arbe, A.; Alegria, A.; Colmenero, J.; Frick, B. *J. Chem. Phys.* **2005**, 123, 014907.
- (66) Liu, S.-F.; Mao, J.-D.; Schmidt-Rohr, K. *J. Magn. Reson.* **2002**, 155, 15–28.
- (67) Graf, R.; Ewen, B.; Spiess, H. W. *J. Chem. Phys.* **2007**, 126, 041104.
- (68) Millward, A. R.; Yaghi, O. M. *J. Am. Chem. Soc.* **2005**, 127, 17998–17999.
- (69) Albulina, A. R.; Graf, R.; Grassi, A.; Guerra, G.; Spiess, H. W. *Macromolecules* **2009**, 42, 4929–4931.
- (70) Qiu, Y.; Park, K. *Adv. Drug Delivery Rev.* **2001**, 53, 321–339.
- (71) Schild, H. G. *Prog. Polym. Sci.* **1992**, 17, 163–249.
- (72) Junk, M. J. N.; Jonas, U.; Hinderberger, D. *Small* **2008**, 4, 1485–1493.
- (73) Keerl, M.; Pedersen, J. S.; Richtering, W. *J. Am. Chem. Soc.* **2009**, 131, 3093–3097.
- (74) Li, W.; Zhang, A.; Feldman, K.; Walde, P.; Schlüter, A. D. *Macromolecules* **2008**, 41, 3659–3667.
- (75) Junk, M. J. N.; Li, W.; Schlüter, A. D.; Wegner, G.; Spiess, H. W.; Zhang, A.; Hinderberger, D. *Angew. Chem., Int. Ed.* **2010**, DOI: 10.1002/anie.201001469.
- (76) Doi, M.; Edwards, S. F. *The Theory of Polymer Dynamics*; Clarendon Press: Oxford, 1986.
- (77) de Gennes, P. G. *J. Chem. Phys.* **1971**, 55, 572–579.
- (78) Rubinstein, M.; Colby, R. H. *Polymer Physics*; Oxford University Press: New York, 2003.
- (79) Milner, S. T.; McLeish, T. C. B. *Phys. Rev. Lett.* **1998**, 81, 725–728.
- (80) Everaers, R.; Sukumaran, S. K.; Grest, G. S.; Svaneborg, C.; Sivasubramanian, A.; Kremer, K. *Science* **2004**, 303, 823–826.
- (81) Pearson, D. S.; Fetters, L. J.; Graessley, W. W.; Strate, G. V.; von Meerwall, E. *Macromolecules* **1994**, 27, 711–719.

- (82) Ball, R. C.; Callaghan, P. T.; Samulski, E. T. *J. Chem. Phys.* **1997**, *106*, 7352–7361.
- (83) Graf, R.; Heuer, A.; Spiess, H. W. *Phys. Rev. Lett.* **1998**, *80*, 5738–5741.
- (84) Herrmann, A.; Novikov, V. N.; Rössler, E. A. *Macromolecules* **2009**, *42*, 2063–2064.
- (85) Chavez, F. A.; Saalwächter, K. *Phys. Rev. Lett.* **2010**, in press.
- (86) Walton, A. G.; Blackwell, J. *Biopolymers*; Academic Press: New York, 1973.
- (87) Klok, H.-A.; Lecommandoux, S. *Adv. Polym. Sci.* **2006**, *202*, 75.
- (88) (a) van Beek, J. D.; Beaulieu, S.; Schafer, L. H.; Demura, M.; Asakura, T.; Meier, B. H. *Nature* **2000**, *405*, 1077–1079. (b) Tycko, R. *Annu. Rev. Phys. Chem.* **2001**, *52*, 575–606.
- (89) Aliferis, T.; Iatrou, H.; Hadjichristidis, N. *Biomacromolecules* **2004**, *5*, 1653–1656.
- (90) Floudas, G.; Spiess, H. W. *Macromol. Rapid Commun.* **2009**, *30*, 278–298.
- (91) Gitsas, A.; Floudas, G.; Mondeshki, M.; Spiess, H. W.; Iatrou, H.; Hadjichristidis, N. *Biomacromolecules* **2008**, *9*, 1959.
- (92) Koynov, K.; Mihov, G.; Mondeshki, M.; Moon, C.; Spiess, H. W.; Müllen, K.; Butt, H.-J.; Floudas, G. *Biomacromolecules* **2007**, *8*, 1745.
- (93) (a) Kreuer, K. D.; Paddison, S. J.; Spohr, E.; Schuster, M. *Chem. Rev.* **2004**, *104*, 4637–4678. (b) Steininger, H.; Schuster, M.; Kreuer, K. D.; Kaltbeitzel, A.; Bingöl, B.; Meyer, W. H.; Schauf, S.; Brunklaus, G.; Maier, J.; Spiess, H. W. *Phys. Chem. Chem. Phys.* **2007**, *9*, 1764–1773.
- (94) Mauritz, K. A.; Moore, R. B. *Chem. Rev.* **2004**, *104*, 4535–4586.
- (95) Schmidt-Rohr, K. *J. Appl. Crystallogr.* **2007**, *40*, 16–25.
- (96) Schmidt-Rohr, K.; Chen, Q. *Nat. Mater.* **2007**, *7*, 75–83.
- (97) Lee, Y. J.; Bingöl, B.; Murakhtina, T.; Sebastiani, D.; Meyer, W. M.; Wegner, G.; Spiess, H. W. *J. Phys. Chem. B* **2007**, *111*, 9711–9721.
- (98) Lee, Y. J.; Murakhtina, T.; Sebastiani, D.; Spiess, H. W. *J. Am. Chem. Soc.* **2007**, *129*, 12406–12407.
- (99) Akbey, Ü.; Granados-Focil, S.; Coughlin, B.; Graf, R.; Spiess, H. W. *J. Phys. Chem. B* **2009**, *113*, 9151–9160.
- (100) Traer, J. W.; Goward, G. R. *Phys. Chem. Chem. Phys.* **2010**, *12*, 263–272.
- (101) Traer, J. W.; Britten, J. F.; Goward, G. R. *J. Phys. Chem. B* **2007**, *111*, 5602–5609.
- (102) Wu, J.; Pisula, W.; Müllen, K. *Chem. Rev.* **2007**, *107*, 718–747.
- (103) Feng, X.; Marcon, V.; Pisula, W.; Hansen, M. R.; Kirkpatrick, J.; Grozema, F.; Andrienko, D.; Kremer, K. *Nat. Mater.* **2009**, *8*, 421–426.
- (104) Schmidt-Mende, L.; Fechtenkötter, A.; Müllen, K.; Moons, E.; Friend, R. H.; MacKenzie, J. D. *Science* **2001**, *293*, 1119–1122.
- (105) Hoebe, F. J. M.; Jonkheijm, P.; Meijer, E. W.; Schenning, A. P. H. *J. Chem. Rev.* **2005**, *105*, 1491–1546.
- (106) Zhang, X.; Chen, Z. J.; Würthner, F. *J. Am. Chem. Soc.* **2007**, *129*, 4886–4887.
- (107) Engelkamp, H.; Middelbeek, S.; Nolte, R. J. M. *Science* **1999**, *284*, 785–788.
- (108) Percec, V.; Imam, M.; Peterca, R. M.; Wilson, D. A.; Graf, R.; Spiess, H. W.; Balagurusamy, V. S. K.; Heiney, P. A. *J. Am. Chem. Soc.* **2009**, *131*, 7662–7677.
- (109) Percec, V.; Glodde, M.; Bera, T. K.; Miura, Y.; Shiyonovskaya, I.; Singer, K. D.; Balagurusamy, V. S. K.; Heiney, P. A.; Schnell, I.; Rapp, A.; Spiess, H. W.; Hudson, S. D.; Duan, H. *Nature* **2002**, *417*, 384–387.
- (110) Goldfarb, D.; Luz, Z. *J. Phys. (Paris)* **1981**, *42*, 1303–1311.
- (111) Leisen, J.; Werth, M.; Boeffel, C.; Spiess, H. W. *J. Chem. Phys.* **1992**, *97*, 3749–3759.
- (112) Vallerien, S. U.; Werth, M.; Kremer, F.; Spiess, H. W. *Liq. Cryst.* **1990**, *8*, 889–893.
- (113) Herwig, P.; Kayser, C. W.; Müllen, K.; Spiess, H. W. *Adv. Mater.* **1996**, *8*, 510–513.
- (114) Mulder, F. M.; Stride, J.; Picken, S. J.; Kouwer, P. H. J.; de Haas, M. P.; Siebbeles, L. D. A.; Kearley, G. J. *J. Am. Chem. Soc.* **2003**, *125*, 3860–3866.
- (115) Kirkpatrick, J.; Marcon, V.; Nelson, J.; Kremer, K.; Andrienko, D. *Phys. Rev. Lett.* **2007**, *98*, 227402.
- (116) Elmahdy, M. M.; Floudas, G.; Mondeshki, M.; Spiess, H. W.; Dou, X.; Müllen, K. *Phys. Rev. Lett.* **2008**, *100*, 107801–4.
- (117) Hansen, M. R.; Graf, R.; Sekharan, S.; Sebastiani, D. *J. Am. Chem. Soc.* **2009**, *131*, 5251–5256.
- (118) Hansen, M. R.; Schnitzler, T.; Pisula, W.; Graf, R.; Müllen, K.; Spiess, H. W. *Angew. Chem., Int. Ed.* **2009**, *48*, 4621–4624.
- (119) Lange, O. F.; Lakomek, N. A.; Fares, C.; Schroeder, G. F.; Walter, K. F. A.; Becker, S.; Meiler, J.; Grubmueller, H.; Griesinger, C.; de Groot, B. L. *Science* **2008**, *320*, 1471–1475.
- (120) Ochsenfeld, C.; Brown, S. P.; Schnell, I.; Gauss, J.; Spiess, H. W. *J. Am. Chem. Soc.* **2001**, *123*, 2597–2606.
- (121) Goward, G. R.; Schuster, M. F. H.; Sebastiani, D.; Schnell, I.; Spiess, H. W. *J. Phys. Chem. B* **2002**, *106*, 9322–9334.
- (122) He, Y. Y.; Lutz, T. R.; Ediger, M. D.; Ayyagari, C.; Bedrov, D.; Smith, G. D. *Macromolecules* **2004**, *37*, 5032–5039.
- (123) Spiess, H. W. *NMR: Basic Princ. Prog.* **1978**, *15*, 55–214.
- (124) Schmidt, J.; Hutter, J.; Spiess, H. W.; Sebastiani, D. *Chem-Phys Chem* **2009**, *9*, 2313–2316.
- (125) Wegner, G. *Macromol. Rapid Commun.* **2009**, *30*, 649–652.
- (126) Segalman, R. A.; McCulloch, B.; Kirmayer, S.; Urban, J. J. *Macromolecules* **2009**, *42*, 9205–9216.
- (127) Jinnai, H.; Spontak, R. J.; Nishi, T. *Macromolecules* **2010**, *43*, 1675–1688.
- (128) Cai, W. Z.; Schmidt-Rohr, K.; Egger, N.; Gerharz, B.; Spiess, H. W. *Polymer* **1993**, *34*, 267–276.
- (129) Chin, Y. H.; Zhang, C.; Wang, P.; Inglefield, P. T.; Jones, A. A.; Kambour, R. P.; Bendler, J. T.; White, D. M. *Macromolecules* **1992**, *25*, 3031–3038.
- (130) Chung, G. C.; Kornfield, J. A.; Smith, S. D. *Macromolecules* **1994**, *27*, 964–973.
- (131) Gill, L.; Damron, J.; Wachowicz, M.; White, J. L. **2010**, *43*, 3903–3910.
- (132) Klok, H. A. *Macromolecules* **2009**, *42*, 7990–8000.
- (133) Cabrita, L. D.; Dobson, C. M.; Christodoulou, J. *Curr. Opin. Struct. Biol.* **2010**, *20*, 33–45.
- (134) (a) Martin, R. E.; Pannier, M.; Diederich, F.; Gramlich, V.; Hubrich, M.; Spiess, H. W. *Angew. Chem., Int. Ed.* **1998**, *37*, 2834–2837. (b) Pannier, M.; Veit, S.; Godt, A.; Jeschke, G.; Spiess, H. W. *J. Magn. Reson.* **2000**, *142*, 331–340.
- (135) Dockter, C.; Volkov, A.; Bauer, C.; Polyhach, Y.; Joly-Lopez, Z.; Jeschke, G.; Paulsen, H. *Proc. Natl. Acad. Sci. U.S.A.* **2009**, *106*, 18491–18496.
- (136) Spiess, H. W. *Angew. Chem., Int. Ed.* **2008**, *47*, 639–642.
- (137) Blanc, F.; Coperet, C.; Thivolle-Cazat, J.; Basset, J. M.; Lesage, A.; Emsley, L.; Sinha, A.; Schrock, R. R. *Angew. Chem., Int. Ed.* **2006**, *45*, 1216–1220.
- (138) Grey, C. P.; Dupré, N. *Chem. Rev.* **2004**, *104*, 4493–4512.
- (139) Yamakawa, N.; Jiang, M.; Key, B.; Grey, C. P. *J. Am. Chem. Soc.* **2009**, *131*, 10525–10536.
- (140) Zauhsail, J.; Friend, R. H.; Sirringhaus, H. *Nat. Mater.* **2006**, *5*, 69–74.
- (141) Laquai, F.; Park, S.; Kim, J. J.; Basché, T. *Macromol. Rapid Commun.* **2009**, *30*, 1203–1231.